

Phase Relations Between Iridium and the Sesquioxides in Air

S. J. Schneider, J. L. Waring, and R. E. Tressler¹

(February 11, 1965)

A study has been made by x-ray diffraction analysis of the reactions that occur in an air environment between Ir and IrO₂ and each of the following: Nd₂O₃, Sm₂O₃, Eu₂O₃, Gd₂O₃, Dy₂O₃, Ho₂O₃, Y₂O₃, Er₂O₃, Tm₂O₃, Yb₂O₃, Lu₂O₃, In₂O₃, Sc₂O₃, and Al₂O₃. In air Ir oxidizes at low temperatures to form IrO₂ which in turn dissociates at 1020 °C. The pseudo binary Nd₂O₃-IrO₂ was studied in detail inasmuch as it typified many of the Ln₂O₃-IrO₂ systems. Two compounds, Nd₂O₃·2IrO₂ and 3Nd₂O₃·2IrO₂ occur in the system. The former, a cubic pyrochlore type phase, dissociates upon heating at 1190 °C. The 3:2 compound dissociates to the solid phases, Nd₂O₃ and Ir, at 1300 °C. Prior to dissociation, the 3:2 compound undergoes an apparent polymorphic transition at 1195 °C which may be related to an oxygen loss. Up to at least 2000 °C no further reaction occurred between Ir and Nd₂O₃. All B- and C-type rare earth oxides formed cubic pyrochlore type compounds with IrO₂. Each of these compounds subsequently dissociated upon heating. No apparent reaction occurred between IrO₂ and either In₂O₃, Sc₂O₃, or Al₂O₃.

1. Introduction

As part of the program at the National Bureau of Standards to obtain accurate melting points of the metal oxides [1]², a study has been initiated to determine what effect, if any, various refractory metal containers have upon possible standard oxides. The type of reaction between appropriate container materials such as iridium (Ir) or tungsten (W) and an oxide can be best characterized through a thorough study of their equilibrium phase relations. As the first in a series of phase equilibria investigations, the present paper reports results obtained in a study of portions of the Nd-Ir-Oxygen and related systems in an air environment.

Preliminary information indicated that powdered Ir has a tendency to oxidize to IrO₂ when heated in air at moderate temperatures. Since complete oxidation is difficult to achieve, IrO₂ rather than Ir metal was selected as one end member of the system. By utilizing IrO₂, an approach to equilibrium could be achieved more readily. The study would still reflect, however, the behavior in air of Ir metal in combination with Nd₂O₃ and other oxides.

Iridium has a face-centered cubic, copper type structure with $a=3.8394$ Å [2]. The freezing point

of Ir is 2443 °C, a value which is given as a secondary reference point on the International Practical Temperature Scale (IPTS)³ [3]. Iridium dioxide (IrO₂) is similar to TiO₂ in having the tetragonal, rutile structure with $a=4.4983$ Å and $c=3.1544$ Å [4]. Upon heating, IrO₂ has been reported to dissociate to the metal and a vapor phase at 1100 °C in one atmosphere oxygen [5].

Neodymium sesquioxide (Nd₂O₃) has been reported to occur in three polymorphic forms; the A, B, and C rare earth oxide structure types [6, 7]. The hexagonal A type ($a=3.831$ Å, $c=5.999$ Å) [8], is generally regarded as the stable modification of Nd₂O₃ although there has been some controversy regarding the existence and stability of the B and C types [6, 7]. The melting point of Nd₂O₃ is not well established. The one value reported in the literature lists the melting point as 2272 °C for material having a purity of 99 percent [9].

Since little data are available on either Ir or IrO₂ in combination with oxides, the present study was broadened somewhat to include, in addition to Nd₂O₃, the following materials: Sm₂O₃, Eu₂O₃, Gd₂O₃, Dy₂O₃, Ho₂O₃, Y₂O₃, Er₂O₃, Tm₂O₃, Yb₂O₃, Lu₂O₃, In₂O₃, Sc₂O₃, and Al₂O₃.

¹ Mr. Tressler is currently a graduate student at Pennsylvania State University.

² Figures in brackets indicate the literature references at the end of this paper.

³ This scale (IPTS) applies to all temperatures listed in this paper.

2. Materials

All starting materials employed in this study had a purity of 99.7 percent or greater. With the exception of Ir, IrO₂, and Al₂O₃, the oxides were used in previous investigations and their spectrochemical analyses are reported elsewhere [10, 11, 12]. The Ir, IrO₂, and Al₂O₃ samples were found by general qualitative spectrochemical analysis⁴ to have the following impurities:

Ir	0.01–0.1% each Pd, Pt and Si; 0.001–0.01% each of Ag, Cu, and Fe; 0.0001–0.001% each Al and Mg; and < 0.0001%, Ca.
IrO ₂	0.01–0.1%, Pt; 0.001–0.01% each Al, Cu, Fe, Pd, and Si; 0.0001–0.001% Mg; and < 0.0001% Ca.
Al ₂ O ₃	0.01–0.1% each Ga, Pb and Si; 0.001–0.01% each Cu, Fe, and Mg; 0.0001–0.001% each Ag, Ca, and Cr.

3. Experimental Procedure

Specimens for the oxide-IrO₂ studies were prepared from 0.5 g batches of various combinations of the end members. Calculated amounts of each oxide, corrected for ignition loss, were weighed to the nearest milligram. Each batch was thoroughly hand mixed, placed in Pt tubes and fired at 800 or 1000 °C a minimum of 19 hr in a muffle furnace.

Following the preliminary heat treatment, a portion of each calcined batch was placed in a small Vycor tube (sealed at one end) and fired in a Pt alloy quench furnace at various temperatures for different periods of time until equilibrium was attained. The Vycor tube containing the specimen was air quenched by quickly pulling the tube from the furnace. Equilibrium was assumed to have been achieved when the x-ray pattern showed no change after successive heat treatments of a specimen or when the data were consistent with the results from a previous set of experiments.

The use of Vycor tubes instead of Pt for experiments above 1000 °C was necessitated by the fact that Ir, frequently found as a decomposition product, readily reacts with Pt. On the other hand, the Vycor tube did not appear to influence or react with the various oxide samples.

Temperatures in the quench furnace, controlled to within ±3 °C, were measured with a 100 percent Pt versus 90 percent Pt–10 percent Rh thermocouple. All reported temperatures pertaining to quench furnace data are considered accurate to within ±5 °C.

⁴The spectrochemical analyses were performed by the Spectrochemical Analysis Section of the National Bureau of Standards.

Several experiments were conducted with mixtures having 1:2 mole ratios of oxide to Ir metal. Specimens of this type were prepared from two gram batches. After each batch was mechanically mixed it was heat treated at three different temperatures; specifically, 1000 °C for 12 hr, 1400 °C for 1 hr and ≈ 2000 °C for 1/2 hr. A small iridium pellet was used as a setter material. A program controlled tube furnace was employed for the 1000 and 1400 °C treatments. An induction furnace [11] utilizing an iridium crucible as both the susceptor and specimen container was used for the 2000 °C treatment. Temperatures were measured with a calibrated optical pyrometer sighted through a small hole in the crucible cover. The optical pyrometer temperature measurements are estimated to be accurate to within ±25 °C or better.

All specimens were examined by x-ray diffraction techniques at room temperature using a high angle recording Geiger counter diffractometer and Ni-filtered Cu radiation.

4. Results and Discussion

4.1. Nd₂O₃–IrO₂ and Nd₂O₃–Ir Systems in Air

The equilibrium phase diagram for the combined Nd₂O₃–IrO₂ and Nd₂O₃–Ir systems in air is given in figure 1. The diagram was constructed from the data listed in table 1. The solid circles indicate the compositions and temperatures of the experiments conducted. It should be emphasized that figure 1 does not represent a true binary system, but a composite of the true binary, Nd₂O₃–Ir, and the pseudo binary, Nd₂O₃–IrO₂, in the Nd–Ir–Oxygen ternary system. At the lower temperatures the oxygen content of the specimens closely conform to the compositions represented by the pseudo binary Nd₂O₃–IrO₂ system. As the temperature is increased, the compositions of the solid phases change by an apparent oxygen loss to those indicated by the Nd₂O₃–Ir join. By considering this dissociation as a type of phase transition in which the vapor phase is ignored, a simple binary representation of the phase relations in a portion of the ternary system can be given. This method of illustration has been employed by a number of investigators, notably A. Muir in his work on iron oxides [13, 14].

At 1020 ± 5 °C in an air environment at atmospheric pressure, IrO₂ was found to dissociate to one solid phase, Ir metal. This value favorably compares with the 1015 °C dissociation temperature at 160 mm Hg oxygen pressure calculated from the data given by Cordfunke and Meyer in their study of the Ir–Oxygen system [5]. The dissociation of IrO₂ is apparently a reversible process. For practical purposes the dissociation can be represented as a type of polymorphic transformation.

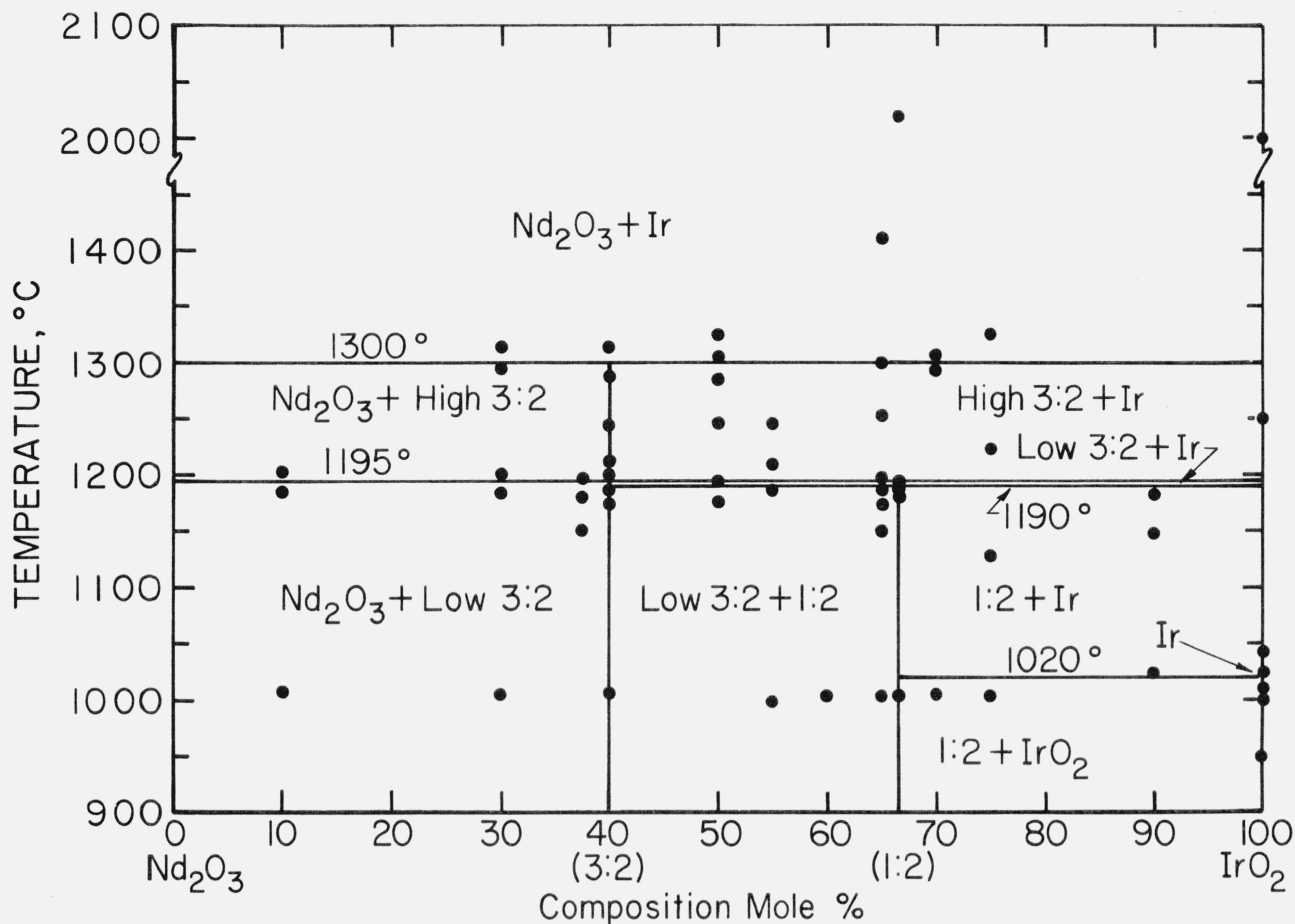


FIGURE 1. Composite phase equilibrium diagrams for the $\text{Nd}_2\text{O}_3\text{-IrO}_2$ and $\text{Nd}_2\text{O}_3\text{-Ir}$ systems in air.

●—compositions and temperatures of experiments conducted in an air environment.

Low 3:2— $3\text{Nd}_2\text{O}_3 \cdot 2\text{IrO}_2$.

High 3:2— $3\text{Nd}_2\text{O}_3 \cdot 2\text{IrO}_2$; x is probably less than 2.

1:2— $\text{Nd}_2\text{O}_3 \cdot 2\text{IrO}_2$ (pyrochlore type compound).

Ir—iridium metal.

TABLE 1. Experimental data for compositions in the $\text{M}_2\text{O}_3\text{-IrO}_2$ and $\text{M}_2\text{O}_3\text{-Ir}$ systems in air

System	Composition	Heat treatment		X-ray diffraction analyses ^b	Remarks
		temp. ^a	Time		
$\text{Nd}_2\text{O}_3\text{-IrO}_2$	Mole % 90:10	1009	19	Nd_2O_3 + low $3\text{Nd}_2\text{O}_3 \cdot 2\text{IrO}_2$	
		1185	19	Nd_2O_3 + low $3\text{Nd}_2\text{O}_3 \cdot 2\text{IrO}_2$	
		1202	20	Nd_2O_3 + high $3\text{Nd}_2\text{O}_3 \cdot 2\text{IrO}_2$	Possibly small amount of low 3:2 present.
	70:30	1009	19	Low $3\text{Nd}_2\text{O}_3 \cdot 2\text{IrO}_2$ + Nd_2O_3	
		1185	60	Low $3\text{Nd}_2\text{O}_3 \cdot 2\text{IrO}_2$ + Nd_2O_3	
		1201	19	Low $3\text{Nd}_2\text{O}_3 \cdot 2\text{IrO}_2$ + high $3\text{Nd}_2\text{O}_3 \cdot 2\text{IrO}_2$ + Nd_2O_3	Nonequilibrium.
		1296	20	High $3\text{Nd}_2\text{O}_3 \cdot 2\text{IrO}_2$ + Nd_2O_3	Possibly small amount of low 3:2 present.
		1315	19	Nd_2O_3 + high $3\text{Nd}_2\text{O}_3 \cdot 2\text{IrO}_2$ + Low $3\text{Nd}_2\text{O}_3 \cdot 2\text{IrO}_2$	Nonequilibrium; low 3:2 probably formed on cooling; Ir not detected by x rays ^d ; high 3:2 present only in minor amounts.

TABLE 1. Experimental data for compositions in the M_2O_3 - IrO_2 and M_2O_3 -Ir systems in air—Continued

System	Composition	Heat treatment		X-ray diffraction analyses ^b	Remarks
		temp. ^a	Time		
Nd ₂ O ₃ -IrO ₂ (cont.)	62.5:37.5	1151	70	Low 3Nd ₂ O ₃ ·2IrO ₂ + Nd ₂ O ₃	Nonequilibrium.
		1180	21	Low 3Nd ₂ O ₃ ·2IrO ₂ + Nd ₂ O ₃	
		1198	22	Low 3Nd ₂ O ₃ ·2IrO ₂ + high 3Nd ₂ O ₃ ·2IrO ₂ + Nd ₂ O ₃	
	60:40 (3:2)	1009	19	Low 3Nd ₂ O ₃ ·2IrO ₂	Nonequilibrium. ^e
		1175	20	Low 3Nd ₂ O ₃ ·2IrO ₂	
		1188	20	Low 3Nd ₂ O ₃ ·2IrO ₂	
		1200	60	Low 3Nd ₂ O ₃ ·2IrO ₂ + high 3Nd ₂ O ₃ ·2IrO ₂ + Nd ₂ O ₃	Possibly some low 3:2 present. Possibly some low 3:2 present. Possibly some low 3:2 present.
	1211	20	High 3Nd ₂ O ₃ ·2IrO ₂		
	1243	20	High 3Nd ₂ O ₃ ·2IrO ₂		
		1290	1.75	High 3Nd ₂ O ₃ ·2IrO ₂	Possibly some low 3:2 present.
	1313	1.75	Nd ₂ O ₃ + Ir		
	50:50	1178	20	Low 3Nd ₂ O ₃ ·2IrO ₂ + Nd ₂ O ₃ ·2IrO ₂	Nonequilibrium; Ir not detected by x rays. ^d
		1195	22	Low 3Nd ₂ O ₃ ·2IrO ₂ + high 3Nd ₂ O ₃ ·2IrO ₂	
		1247	16	High 3Nd ₂ O ₃ ·2IrO ₂ + Ir	
		1289	3	High 3Nd ₂ O ₃ ·2IrO ₂ + Ir	Nonequilibrium. Ir not detected by x rays. ^d
	1305	1.75	High 3Nd ₂ O ₃ ·2IrO ₂ + Nd ₂ O ₃ + Ir		
	1325	5	Nd ₂ O ₃		
	45:55	1000	19	Nd ₂ O ₃ ·2IrO ₂ + low 3Nd ₂ O ₃ ·2IrO ₂	Ir not detected by x rays. ^d Ir not detected by x rays. ^d
		1188	20	Nd ₂ O ₃ ·2IrO ₂ + low 3Nd ₂ O ₃ ·2IrO ₂	
		1210	68	High 3Nd ₂ O ₃ ·2IrO ₂	
		1249	20	High 3Nd ₂ O ₃ ·2IrO ₂	
	40:60	1005	20	Nd ₂ O ₃ ·2IrO ₂ + low 3Nd ₂ O ₃ ·2IrO ₂	Possibly small amount of high 3:2 present. Nonequilibrium; Ir not detected by x rays. ^d Reheat of 1173 °C specimen.
	35:65	1005	20	Nd ₂ O ₃ ·2IrO ₂ + low 3Nd ₂ O ₃ ·2IrO ₂	
		1151	19	Nd ₂ O ₃ ·2IrO ₂ + low 3Nd ₂ O ₃ ·2IrO ₂	
		1173	22	Nd ₂ O ₃ ·2IrO ₂ + low 3Nd ₂ O ₃ ·2IrO ₂	
		1187	17.5	Nd ₂ O ₃ ·2IrO ₂ + low 3Nd ₂ O ₃ ·2IrO ₂	
		1198	17.5	Nd ₂ O ₃ ·2IrO ₂ + low 3Nd ₂ O ₃ ·2IrO ₂ + high 3Nd ₂ O ₃ ·2IrO ₂	
		1253	16	High 3Nd ₂ O ₃ ·2IrO ₂ + Ir	
		1300	3	High 3Nd ₂ O ₃ ·2IrO ₂ + Ir	
		1411	1	Ir + Nd ₂ O ₃	
	33.3:66.7 (1:2)	1005	19	Nd ₂ O ₃ ·2IrO ₂	
		1180	90	Nd ₂ O ₃ ·2IrO ₂ + low 3Nd ₂ O ₃ ·2IrO ₂	
		1189	42	Nd ₂ O ₃ ·2IrO ₂ + low 3Nd ₂ O ₃ ·2IrO ₂	
	30:70	1191	20	Nd ₂ O ₃ ·2IrO ₂ + Ir + low 3Nd ₂ O ₃ ·2IrO ₂	Nonequilibrium.
		1007	18	Nd ₂ O ₃ ·2IrO ₂ + IrO ₂	
		1295	19	High 3Nd ₂ O ₃ ·2IrO ₂ + Ir	
		1308	19	Nd ₂ O ₃ + Ir + high 3Nd ₂ O ₃ ·2IrO ₂	
	25:75	1005	19	Nd ₂ O ₃ ·2IrO ₂ + IrO ₂	Nonequilibrium.
		1030	92	Nd ₂ O ₃ ·2IrO ₂ + Ir	
		1226	16	Low 3Nd ₂ O ₃ ·2IrO ₂	
		1325	4.5	Ir + high 3Nd ₂ O ₃ ·2IrO ₂ + Ir + Nd ₂ O ₃	
	10:90	1027	5	Nd ₂ O ₃ ·2IrO ₂ + Ir + IrO ₂	Nonequilibrium. Nonequilibrium.
		1150	16	Nd ₂ O ₃ ·2IrO ₂ + Ir + IrO ₂	
		1181	67	Nd ₂ O ₃ ·2IrO ₂ + Ir	
	0-100	0	0	Amorphous to x rays	"As received" material. Nonequilibrium. Nonequilibrium.
950		16	IrO ₂		
1010		64	IrO ₂		
1011		16	IrO ₂		
1017		16	IrO ₂		
1018		18	IrO ₂		
1022		16	IrO ₂ + Ir		
1026		3	IrO ₂ + Ir		
1047		12	Ir		
2000		0.5	Ir		
Sm ₂ O ₃ -IrO ₂		33.3:66.7 (1:2)	1000	100	
	1205		19	Sm ₂ O ₃ ·2IrO ₂	
	1216		19	Sm ₂ O ₃ ·2IrO ₂ + unknown phase	
	1229	19	Sm ₂ O ₃ ·2IrO ₂ + Ir + unknown phase	Nonequilibrium; unknown phase similar to low 3Nd ₂ O ₃ ·2IrO ₂ .	

TABLE 1. Experimental data for compositions in the M_2O_3 - IrO_2 and M_2O_3 -Ir systems in air—Continued

System	Composition	Heat treatment		X-ray diffraction analyses ^b	Remarks
		temp. ^a	Time		
Eu_2O_3 - IrO_2	33.3:66.7 (1:2)	1000	100	$Eu_2O_3 \cdot 2IrO_2$	Nonequilibrium; Ir not detected by x ray. ^d Nonequilibrium; Ir not detected by x ray. ^d
		†1207	64	$Eu_2O_3 \cdot 2IrO_2$	
		†1215	64	$Eu_2O_3 \cdot 2IrO_2$	
		†1225	16	$Eu_2O_3 \cdot 2IrO_2$ + unknown phase	
		†1231	16	$Eu_2O_3 \cdot 2IrO_2$ + unknown phase	
	†1346	19	Eu_2O_3 + Ir		
Gd_2O_3 - IrO_2	33.3:66.7 (1:2)	1000	100	$Gd_2O_3 \cdot 2IrO_2$ + Gd_2O_3	Nonequilibrium. ^e
		†1218	19	$Gd_2O_3 \cdot 2IrO_2$ + Gd_2O_3	Nonequilibrium. ^e
		†1235	19	$Gd_2O_3 \cdot 2IrO_2$ + Gd_2O_3	Nonequilibrium. ^e
		†1242	19	$Gd_2O_3 \cdot 2IrO_2$ + Gd_2O_3 + Ir	Nonequilibrium. ^e
Dy_2O_3 - IrO_2	33.3:66.7 (1:2)	†1000	100	$Dy_2O_3 \cdot 2IrO_2$ + Dy_2O_3	Nonequilibrium. ^e
		†1170	92	$Dy_2O_3 \cdot 2IrO_2$ + Dy_2O_3	Nonequilibrium. ^e
		†1200	19	$Dy_2O_3 \cdot 2IrO_2$ + Dy_2O_3	Nonequilibrium. ^e
		†1242	19	$Dy_2O_3 \cdot 2IrO_2$ + Dy_2O_3	Nonequilibrium. ^e
		†1260	20	$Dy_2O_3 \cdot 2IrO_2$ + Dy_2O_3 + unknown phase	Nonequilibrium. ^e
		†1301	4	$Dy_2O_3 \cdot 2IrO_2$ + Dy_2O_3 + unknown phase	Nonequilibrium. ^e
	†1351	19	Dy_2O_3 + Ir		
Ho_2O_3 - IrO_2	33.3:66.7 (1:2)	1000	100	$Ho_2O_3 \cdot 2IrO_2$ + Ho_2O_3 + IrO_2	Nonequilibrium.
		†1218	19	$Ho_2O_3 \cdot 2IrO_2$ + Ho_2O_3	Nonequilibrium. ^e
		†1235	19	$Ho_2O_3 \cdot 2IrO_2$ + Ho_2O_3 + Ir	Nonequilibrium. ^e
Y_2O_3 - IrO_2	33.3:66.7 (1:2)	1000	100	$Y_2O_3 \cdot 2IrO_2$ + Y_2O_3	Nonequilibrium. ^e
		†1210	19	$Y_2O_3 \cdot 2IrO_2$ + Y_2O_3	Nonequilibrium. ^e
		†1216	4	$Y_2O_3 \cdot 2IrO_2$ + Y_2O_3	Nonequilibrium. ^e
		1225	19	$Y_2O_3 \cdot 2IrO_2$ + Y_2O_3 + unknown phase	Nonequilibrium. ^e
		1351	19	Y_2O_3 + Ir	
Er_2O_3 - IrO_2	33.3:66.7 (1:2)	1000	100	$Er_2O_3 \cdot 2IrO_2$ + Er_2O_3	Nonequilibrium. ^e
		†1215	64	$Er_2O_3 \cdot 2IrO_2$ + Er_2O_3	Nonequilibrium. ^e
		†1225	64	$Er_2O_3 \cdot 2IrO_2$ + Er_2O_3	Nonequilibrium. ^e ; 1:2 phase reduced in amount from that of previous heat treatment. Ir not detected by x rays. ^d
		1346	19	Er_2O_3 + Ir	
Tm_2O_3 - IrO_2	33.3:66.7 (1:2)	1000	100	$Tm_2O_3 \cdot 2IrO_2$ + Tm_2O_3	Nonequilibrium. ^e
		†1199	19	$Tm_2O_3 \cdot 2IrO_2$ + Tm_2O_3	Nonequilibrium. ^e
		†1226	19	$Tm_2O_3 \cdot 2IrO_2$ + Tm_2O_3	Nonequilibrium. ^e ; 1:2 phase reduced in amount from that of previous heat treatment; Ir not detected by x rays. ^d
		1351	19	Tm_2O_3 + Ir	
Yb_2O_3 - IrO_2	33.3:66.7 (1:2)	1000	100	$Yb_2O_3 \cdot 2IrO_2$ + Yb_2O_3	Nonequilibrium. ^e
		†1161	19	$Yb_2O_3 \cdot 2IrO_2$ + Yb_2O_3	Nonequilibrium. ^e
		†1173	19	$Yb_2O_3 \cdot 2IrO_2$ + Yb_2O_3	Nonequilibrium. ^e
		†1199	19	$Yb_2O_3 \cdot 2IrO_2$ + $Yb_2O_3 \cdot 2IrO_2$	Nonequilibrium.
		†1226	19	Yb_2O_3 + Ir	
Lu_2O_3 - IrO_2	33.3:66.7 (1:2)	1000	100	$Lu_2O_3 \cdot 2IrO_2$ + Lu_2O_3	Nonequilibrium. ^e
		†1161	19	$Lu_2O_3 \cdot 2IrO_2$ + Lu_2O_3	Nonequilibrium. ^e
		†1170	19	$Lu_2O_3 \cdot 2IrO_2$ + Lu_2O_3	Nonequilibrium. ^e ; 1:2 phase reduced in amount from that of previous heat treatment; Ir not detected by x rays. ^d
		†1200	19	Lu_2O_3 + Ir + $Lu_2O_3 \cdot 2IrO_2$	Nonequilibrium.
	†1309	19	Lu_2O_3 + Ir		
In_2O_3 - IrO_2	33.3:66.7 (1:2)	1000	100	In_2O_3 + IrO_2	
		1256	19	In_2O_3 + Ir	
Sc_2O_3 - IrO_2	33.3:66.7 (1:2)	1000	100	Sc_2O_3 + IrO_2	Ir not detected by x rays. ^d
		1256	19	Sc_2O_3	
Al_2O_3 - IrO_2	33.3:66.7 (1:2)	1000	100	Al_2O_3 + IrO_2	
		1256	19	Al_2O_3 + Ir	
Nd_2O_3 -Ir	33.3:66.7 (1:2)	1000	12	$Nd_2O_3 \cdot 2IrO_2$ + Ir + IrO_2	Nonequilibrium.
		†1400	1	Ir + Nd_2O_3 + $Nd(OH)_3$	Nd_2O_3 commonly hydrates at room temperature.
		†2020	.75	Ir + Nd_2O_3 + $Nd(OH)_3$	Nd_2O_3 commonly hydrates at room temperature.

TABLE 1. Experimental data for compositions in the M_2O_3 - IrO_2 and M_2O_3 -Ir systems in air—Continued

System	Composition	Heat treatment		X-ray diffraction analyses ^b	Remarks
		temp. ^a	Time		
Nd ₂ O ₃ -Ir (cont.)	0:100	0	0	Ir	"As received." Nonequilibrium. Nonequilibrium; greater amount of IrO ₂ present from that of previous heat treatment. Nonequilibrium. Nonequilibrium; smaller amount of IrO ₂ present from that of previous heat treatment. Nonequilibrium; only small amount of IrO ₂ present. IrO ₂ probably formed on cooling.
		1000	6	IrO ₂ + Ir	
		^c 1000	20	IrO ₂ + Ir	
		^c 1000	116	IrO ₂ + Ir	
		^c 1040	18	Ir + IrO ₂	
Sm ₂ O ₃ -Ir	33.3:66.7 (1:2)	1000	12	Sm ₂ O ₃ ·2IrO ₂ + IrO ₂ + Ir + unknown phase	Nonequilibrium; unknown phase similar to low 3Nd ₂ O ₃ ·2IrO ₂ .
		^c 1400	1	Sm ₂ O ₃ + Ir	
		^c 2030	0.50	Sm ₂ O ₃ + Ir	
Eu ₂ O ₃ -Ir	33.3:66.7 (1:2)	1000	12	Eu ₂ O ₃ ·2IrO ₂	
		^c 1400	1	Eu ₂ O ₃ + Ir	
		^c 2020	0.50	Eu ₂ O ₃ + Ir	
Gd ₂ O ₃ -Ir	33.3:66.7 (1:2)	1000	12	Gd ₂ O ₃ ·2IrO ₂ + Gd ₂ O ₃ + IrO ₂ + Ir	Nonequilibrium.
		^c 1400	1	Gd ₂ O ₃ + Ir	
		^c 2015	0.50	Gd ₂ O ₃ + Ir	
Dy ₂ O ₃ -Ir	33.3:66.7 (1:2)	1000	12	Dy ₂ O ₃ ·2IrO ₂ + Dy ₂ O ₃ + IrO ₂ + Ir	Nonequilibrium.
		^c 1400	1	Dy ₂ O ₃ + Ir	
		^c 2015	0.50	Dy ₂ O ₃ + Ir	
Y ₂ O ₃ -Ir	33.3:66.7 (1:2)	1000	12	Y ₂ O ₃ ·2IrO ₂ + Y ₂ O ₃ + IrO ₂ + Ir	Nonequilibrium.
		^c 1400	1	Y ₂ O ₃ + Ir	
		2010	0.50	Y ₂ O ₃ + Ir	
Lu ₂ O ₃ -Ir	33.3:66.7 (1:2)	1000	12	Lu ₂ O ₃ ·2IrO ₂ + Lu ₂ O ₃ + IrO ₂ + Ir	Nonequilibrium.
		^c 1400	1	Lu ₂ O ₃ + Ir	
		^c 2080	0.50	Lu ₂ O ₃ + Ir	
Al ₂ O ₃ -Ir	33.3:66.7 (1:2)	1000	12	Al ₂ O ₃ + Ir + IrO ₂	Nonequilibrium. Nonequilibrium; IrO ₂ probably formed on cooling. Specimen partially melted.
		^c 1400	1	Al ₂ O ₃ + Ir	
		2010	0.5	Al ₂ O ₃ + Ir + IrO ₂	
		2055	0.5	Al ₂ O ₃ + Ir	

^a All specimens in the Nd₂O₃-IrO₂ system heat treated at 800 °C a minimum of 24 hrs prior to the listed heat treatment.

^b The phases identified are given in order of the relative amount present at room temperature.

^c Reheat of the previous specimen.

^d Iridium dioxide (IrO₂) in combination with other oxides, upon

dissociation, forms small Ir metal grains which are generally detectable by microscopic examination. X-ray patterns of these specimens often fail to show reflections representing Ir unless there is anomalous intensity due to orientation of the grains.

^e Small amount of IrO₂ probably lost by volatilization.

^f Reheat of 1000 °C specimen.

As IrO₂ is heated to temperatures near its dissociation temperature, it becomes somewhat volatile. Cordfunke and Meyer [5] conclude that IrO₂ combines with oxygen to form IrO₃ which is stable only in the gaseous state. Efforts to produce solid IrO₃ in the present work proved unsuccessful. The condensed vapors from heated samples of either IrO₂ or Ir always were identified as IrO₂. The problem of the volatility of IrO₂ in the present study was minimized greatly by reacting the end members at low temperatures. The volatilization of IrO₂ was sufficiently inhibited by re-

action to consider the listed compositions (cation to metal ratio) of table 1 as being near correct.

Two intermediate binary compounds occur in the Nd₂O₃-IrO₂ system. One phase, a 1:2 compound, is stable up to 1190 °C where it dissociates to two solid phases and a vapor phase, presumably oxygen. The composition of the 1:2 compound corresponds to that of an A₂B₂O₇ pyrochlore type phase. Table 2 gives the x-ray pattern of Nd₂O₃·2IrO₂ indexed on the basis of the typical face-centered cubic symmetry ($a = 10.383\text{\AA}$) of the pyrochlore structure.

TABLE 2. X-ray diffraction powder data for $\text{Nd}_2\text{O}_3 \cdot 2\text{IrO}_2$ (CuK α radiation)^a

hkl^b	d^c	I/I_0^d
111	6.00	6
311	3.140	4
222	3.003	100
400	2.673	43
511/333	2.0035	3
440	1.8370	46
622	1.5661	40
444	1.4994	11
800	1.2986	6
622	1.1913	11
840	1.1613	10
844	1.0601	9
10,22/666	0.9995	9
880	.9174	3
11,33/973	.8813	3
10,62	.8772	9
12,00/884	.8652	9
12,40	.8205	3

^a X-ray pattern obtained from specimen heat treated at 1005 °C for 19 hrs in air.

^b The Miller indices are those representing a fcc unit cell with $a=10.383$ Å.

^c Interplanar spacing.

^d Relative Intensity.

The other binary phase was found to occur in the system at the 3:2 composition. This compound, $3\text{Nd}_2\text{O}_3 \cdot 2\text{IrO}_2$, similar in behavior to the 1:2 phase, also dissociates to two solid phases (and vapor) at 1300 °C. At 1195 °C, the 3:2 compound appears to undergo a polymorphic transformation. The unindexed x-ray powder patterns of both the high and low forms are given in table 3. Because the transformation temperature of the 3:2 compound and the dissociation temperature of the 1:2 phase are approximately the same, it appears likely that an oxygen loss may have produced the apparent polymorphic phase change. Therefore, the phase designated high 3:2 in figure 1, may be, in reality, an oxygen deficient phase, $3\text{Nd}_2\text{O}_3 \cdot 2\text{IrO}_x$, where x is less than 2.

At temperatures above 1300 °C the system under consideration no longer can be represented by the pseudo system, $\text{Nd}_2\text{O}_3\text{-IrO}_2$. Through dissociation, the system had changed to the $\text{Nd}_2\text{O}_3\text{-Ir}$ binary. Up to temperatures of 2000 °C, Nd_2O_3 and Ir do not react in the solid state. Presumably no solid state reaction would occur below melting. No definite conclusions can be made concerning the melting characteristics of the system until further experimental work has been performed.

It should be noted that figure 1 pertains only to the phase relations of the system in an air environment at atmospheric pressure. Any change in oxygen pressure would greatly change the diagram. To emphasize this, limited experiments were carried out utilizing sealed Pt tubes as containers. In every instance the pressure in the tube was sufficient to raise the temperatures of dissociation of mixtures of the compounds with IrO_2 20 to 150 °C. For unexplained reasons pure

IrO_2 could not be heated to temperatures in excess of 1000 °C without tube failure due to the high internal pressure.

TABLE 3. X-ray diffraction powder data for the "high" and "low" forms of $3\text{Nd}_2\text{O}_3 \cdot 2\text{IrO}_2$ (CuK α radiation)^a

"Low" $3\text{Nd}_2\text{O}_3 \cdot 2\text{IrO}_2^b$		"High" $3\text{Nd}_2\text{O}_3 \cdot 2\text{IrO}_2^c$	
d^d	I/I_0^e	d^d	I/I_0^e
3.34	11	4.65	7
3.20	100	4.06	32
3.00	11	4.02	11
2.85	16	3.70	4
2.73	18	3.28	8
2.64	34	3.12	7
2.379	5	3.09	28
2.199	5	2.85	100
2.110	6	2.84	56
2.076	5	2.72	4
2.050	4	2.57	4
2.013	5	2.494	7
1.940	5	2.443	13
1.897	36	2.424	13
1.875	11	2.418	8
1.840	4	2.110	7
1.808	3	2.091	18
1.763	5	2.030	13
1.725	6	2.005	28
1.633	13		
1.601	18		
1.596	16		
1.545	10		

^a The x-ray patterns of these specimens show only broad and generally weak peaks. Therefore, only the more intense, readily measurable reflections are reported.

^b X-ray pattern obtained from specimen heat treated at 1009 °C for 19 hrs in air.

^c X-ray pattern obtained from specimen heat treated at 1243 °C for 20 hrs in air. The high form may be oxygen deficient with the formula corresponding to the type $3\text{Nd}_2\text{O}_3 \cdot 2\text{IrO}_x$ where x is less than two.

^d Interplanar Spacing.

^e Relative Intensity.

4.2. Other $\text{M}_2\text{O}_3\text{-IrO}_2$ Systems in Air

Montmony and Bertaut [15] have previously reported the existence of pyrochlore type compounds in mixtures of rare earth sesquioxides and IrO_2 . In order to confirm the earlier work and to investigate these compounds more fully, $\text{M}_2\text{O}_3:2\text{IrO}_2$ mole ratio mixtures were prepared from IrO_2 and either Sm_2O_3 , Eu_2O_3 , Gd_2O_3 , Dy_2O_3 , Ho_2O_3 , Y_2O_3 , Er_2O_3 , Tm_2O_3 , Yb_2O_3 , Lu_2O_3 , In_2O_3 , Sc_2O_3 , and Al_2O_3 .

Tables 1 and 4 summarize the results obtained for this set of experiments. All 1:2 mixtures containing the rare earth oxides and Y_2O_3 formed face-centered cubic pyrochlore type compounds. Unfortunately, some of the compositions contained, in addition to the pyrochlore type phase, small amounts of the pure rare earth oxide. In all probability an unknown quantity of IrO_2 was lost by volatilization before complete combination occurred. The possibility still remains, however, that the true composition of the pyrochlore phase does not correspond to the idealized $\text{Ln}_2\text{Ir}_2\text{O}_7$ formula. Evidence for "off composition" pyrochlore compounds have been reported elsewhere [16].

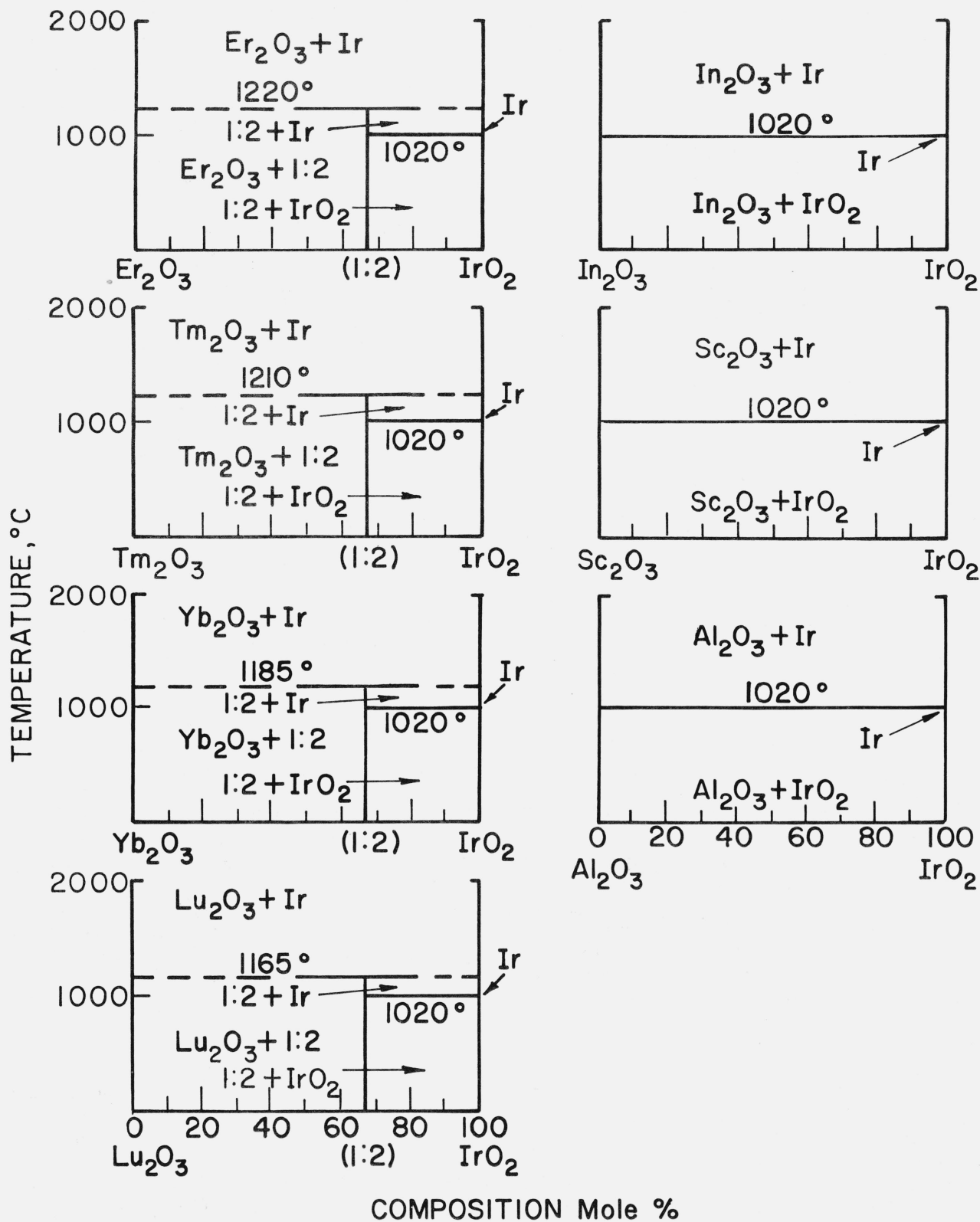


FIGURE 2. Predicted composite phase equilibrium diagrams for various M_2O_3 - IrO_2 and M_2O_3 -Ir systems in air.

For clarity experimental points are not included. See table 1 for exact compositions and temperatures studied. All experiments conducted involved only the $M_2O_3:2IrO_2$ compositions in an air environment. Ir—Iridium metal, 1:2- $M_2O_3 \cdot 2IrO_2$.

As expected, the unit cell dimensions of the cubic pyrochlore compounds decrease in a linear manner as the size of the rare earth cation decreases. In a manner similar to $\text{Nd}_2\text{Ir}_2\text{O}_7$, all the compounds dissociated at temperatures above 1020 °C, the decomposition temperature of IrO_2 . The dissociation temperatures (table 4) when plotted as a function of the radius of the rare earth cation do not change linearly as do the unit cell dimensions. As the size of the cation is decreased, the dissociation temperature at first increases, approaching a maximum for $\text{Dy}_2\text{Ir}_2\text{O}_7$ and then decreases to a minimum for $\text{Lu}_2\text{Ir}_2\text{O}_7$.

Under the conditions of the experiments In_2O_3 , Sc_2O_3 , and Al_2O_3 did not react even partially with IrO_2 . X-ray patterns of these mixtures after heat treatment at 1000 °C show only reflections representing IrO_2 and the admixture oxide. Additional heat treatment at 1256 °C failed to cause combination and only succeeded in dissociating the IrO_2 . The resultant mixture contained the refractory oxide and Ir metal.

It is evident that the $\text{Nd}_2\text{O}_3\text{-IrO}_2$ system is representative in a general way of the other $\text{M}_2\text{O}_3\text{-IrO}_2$ systems. Using it as a guide, figure 2 gives a number of the sub-solidus phase diagrams for various systems as predicted from the data tabulated in table 1.

The $\text{In}_2\text{O}_3\text{-IrO}_2$, $\text{Sc}_2\text{O}_3\text{-IrO}_2$, and $\text{Al}_2\text{O}_3\text{-IrO}_2$ systems are rather simple and straightforward inasmuch as there is no detectable reaction between end members in the solid state. These diagrams indicate only the dissociation of IrO_2 , the point at which the system reverts to the true $\text{M}_2\text{O}_3\text{-Ir}$ system.

The diagrams for the $\text{Er}_2\text{O}_3\text{-IrO}_2$, $\text{Tm}_2\text{O}_3\text{-IrO}_2$, $\text{Yb}_2\text{O}_3\text{-IrO}_2$, and $\text{Lu}_2\text{O}_3\text{-IrO}_2$ systems in air are slightly more complicated, each indicating the occurrence of a 1:2 compound. Studies of 1:2 compounds show that they dissociate to the solid phases M_2O_3 and Ir. If other phases occurred in the systems, they necessarily would have to dissociate at lower temperatures than the 1:2 compound. If other compounds existed which were stable at temperatures greater than the 1:2 dissociation temperatures, they would appear as a decomposition product of the pyrochlore type phase. As stated previously, this was not the case. On the basis of the more complete $\text{Nd}_2\text{O}_3\text{-IrO}_2$ study, the existence of phases other than the 1:2 is not considered likely for these systems.

Additional experimentation is needed before the $\text{Sm}_2\text{O}_3\text{-IrO}_2$, $\text{Eu}_2\text{O}_3\text{-IrO}_2$, $\text{Gd}_2\text{O}_3\text{-IrO}_2$, $\text{Dy}_2\text{O}_3\text{-IrO}_2$, $\text{Ho}_2\text{O}_3\text{-IrO}_2$, and $\text{Y}_2\text{O}_3\text{-IrO}_2$ systems can be drawn. Each of the 1:2 compounds occurring in these systems dissociates to a mixture of solid phases, generally consisting of Ir and an unidentified phase.

4.3. $\text{M}_2\text{O}_3\text{-Ir}$ Reactions

In order to establish whether or not the results found

for the $\text{M}_2\text{O}_3\text{-IrO}_2$ studies were indicative of Ir in combination with various oxides, a limited number of experiments were performed involving oxide-Ir mixtures. Table 1 gives the data obtained for 1:2 mole ratio (oxide:metal) mixtures heat treated in an air environment. It is apparent that Ir oxidizes at least partially to IrO_2 , which, in turn reacts with the admixture oxide to form the same pyrochlore type compounds listed in table 4. At higher temperatures the pyrochlore type compounds dissociated as expected and further reaction between end members did not take place.

TABLE 4. $\text{Ln}_2\text{O}_3 \cdot 2\text{IrO}_2$ pyrochlore-type compounds

Compound	Radius of Ln^{+3} ^a	Dissociation temperature ^b	X-ray data	
			Symmetry	Unit cell dimension
	Å	°C		Å
$\text{Nd}_2\text{O}_3 \cdot 2\text{IrO}_2$	1.04	1190	cubic	10.383
$\text{Sm}_2\text{O}_3 \cdot 2\text{IrO}_2$	1.00	1210	cubic	10.313
$\text{Eu}_2\text{O}_3 \cdot 2\text{IrO}_2$	0.98	1220	cubic	10.293
$\text{Gd}_2\text{O}_3 \cdot 2\text{IrO}_2$.97	1240	cubic	10.265
$\text{Dy}_2\text{O}_3 \cdot 2\text{IrO}_2$.92	1250	cubic	10.207
$\text{Ho}_2\text{O}_3 \cdot 2\text{IrO}_2$.91	1225	cubic	10.180
$\text{Y}_2\text{O}_3 \cdot 2\text{IrO}_2$	=.91	1220	cubic	10.177
$\text{Er}_2\text{O}_3 \cdot 2\text{IrO}_2$.89	1220	cubic	10.163
$\text{Tm}_2\text{O}_3 \cdot 2\text{IrO}_2$.87	1210	cubic	10.134
$\text{Yb}_2\text{O}_3 \cdot 2\text{IrO}_2$.86	1185	cubic	10.115
$\text{Lu}_2\text{O}_3 \cdot 2\text{IrO}_2$.85	1165	cubic	10.096

^a All radii of the rare earth cations taken from Arhens [17] with the exception of Y^{+3} which was estimated by Roth and Schneider [4].

^b Dissociation temperatures are applicable only to those specimens heated in air.

Unfortunately, Ir either alone or in combination with an oxide, never completely oxidized to IrO_2 . As indicated by microscopic examination, IrO_2 , as it forms, appears to coat the Ir grains and thus tends to inhibit additional oxidation. At temperatures just below the IrO_2 dissociation temperature, IrO_2 is somewhat volatile. As the metal forms IrO_2 , the oxide is lost by vaporization and a steady state is reached where the metal:oxide (Ir: IrO_2) ratio of the remaining material appears to remain approximately constant. In essence, true equilibrium at low temperatures could not be obtained in the $\text{M}_2\text{O}_3 \cdot 2\text{Ir}$ mixtures because of the inherent difficulty in achieving complete oxidation of Ir. Except for the presence of Ir at low temperatures, the data for the $\text{M}_2\text{O}_3 \cdot 2\text{Ir}$ compositions completely substantiated the $\text{M}_2\text{O}_3\text{-IrO}_2$ studies. Also, these data, in effect, establish the reversibility of the various transformations (dissociation) discussed earlier.

In all the aforementioned experiments, every effort was made through thorough mixing and prolonged heat treatment to react Ir with the various oxides. Even with these precautions, Ir while in the metallic state appears to be unreactive with the oxides studied and thus seems quite acceptable as a container material for high temperature application in an air environment.

The fact that Ir oxidizes at low temperatures does not appreciably detract from its use as a container since all phases containing IrO_2 subsequently dissociate.

4.4. Summary

Selected mixtures in systems involving Ir or IrO_2 and various sesquioxides were studied by x-ray diffraction techniques after heat treatment in an air environment. Iridium, in air, oxidizes almost completely to IrO_2 at low temperatures. The dissociation temperature of IrO_2 in air at atmospheric pressure was established at 1020 ± 5 °C. Iridium in combination with the sesquioxides also forms IrO_2 which in turn reacts with a number of the oxides to form binary compounds. The pseudo binary system $\text{Nd}_2\text{O}_3\text{-IrO}_2$ exemplified the typical type of reaction and was studied in detail. Two phases, a compound believed to be $3\text{Nd}_2\text{O}_3 \cdot 2\text{IrO}_2$ having unknown symmetry and a cubic pyrochlore type compound $\text{Nd}_2\text{O}_3 \cdot 2\text{IrO}_2$, with $a = 10.383$ Å, occur in the system. The 3:2 and 1:2 compounds dissociate at 1300 and 1190 °C respectively. Above 1300 °C the system corresponds to the $\text{Nd}_2\text{O}_3\text{-Ir}$ join in the Nd-Ir-O ternary system. No further reaction appears to take place between Nd_2O_3 and Ir up to 2000 °C.

Pyrochlore type compounds also were found to occur at the 1:2 mixture of either Sm_2O_3 , Eu_2O_3 , Gd_2O_3 , Ho_2O_3 , Y_2O_3 , Dy_2O_3 , Er_2O_3 , Tm_2O_3 , Yb_2O_3 , or Lu_2O_3 with IrO_2 . Each of these compounds also dissociated upon heating at temperatures above the dissociation temperature of IrO_2 . Mixtures of either In_2O_3 , Sc_2O_3 , or Al_2O_3 with IrO_2 did not react at temperatures up to 2000 °C. The phase diagrams for a number of the $\text{M}_2\text{O}_3\text{-IrO}_2$ systems have been predicted.

5. References

- [1] S. J. Schneider, *Mono.* 68, NBS, 31 p. (1963).
- [2] H. E. Swanson, R. K. Fuyat and G. M. Ugrinic, *NBS Cir.* 539, **4**, 9-10 (1963).
- [3] H. F. Stimson, *J. Res. NBS* **65A** (Phys. and Chem.) No. 3, 139-145 (1960).
- [4] H. E. Swanson, M. C. Morris and E. H. Evans, *NBS Mono.* 25, Sec. 4 (1965) to be published.
- [5] E. H. P. Cordfunke and G. Meyer, *Rec. Trav. Chim.* **81**, 495-504 (1962).
- [6] R. S. Roth and S. J. Schneider, *J. Res. NBS* **64A** (Phys. and Chem.) No. 4, 309-318 (1960).
- [7] M. W. Shafer and R. Roy, *J. Am. Ceram. Soc.* **42**, 563-570 (1959).
- [8] H. E. Swanson, R. K. Fuyat and G. M. Ugrinic, *NBS Cir.* 539, **4**, 26 (1963).
- [9] W. A. Lambertson and F. H. Gunzel, Jr., *A.N.L. U.S. AEC Publ. AEC-D-3465*, 1-4 (1952).
- [10] S. J. Schneider and R. S. Roth, *J. Res. NBS* **65A** (Phys. and Chem.) No. 4, 317-332 (1960).
- [11] S. J. Schneider, *J. Res. NBS* **65A** (Phys. and Chem.) No. 5, 429-434 (1961).
- [12] S. J. Schneider and J. L. Waring, *J. Res. NBS* **67A** (Phys. and Chem.) No. 1, 19-25 (1963).
- [13] A. Muan, *Am. J. Sci.* **256** 171-207 (1958).
- [14] A. Muan and C. L. Gee, *J. Am. Ceram. Soc.* **39** (6) 207-214 (1956).
- [15] M. Montmony and F. Bertaut, *Compt. Rend.* **252** 4171-4173 (1961).
- [16] R. S. Roth, *J. Res. NBS* **62A** (Phys. and Chem.) No. 1, 27-38 (1959).
- [17] L. H. Ahrens, *Geochim. et Cosmochim. Acta* **2** 155-169 (1952).

(Paper 69A3-343)